Fizika Nizkikh Temperatur, 2007, v. 33, Nos. 6/7, p. 790–797

Quantitative evaluation of the effects of positional versus orientational disorder on the scattering of acoustic phonons in disordered matter

F.J. Bermejo, R. Fernández-Perea, and C. Cabrillo

Instituto de Estructura de la Materia, CSIC, and Dept. Electricidad y Electrónica-Unidad Asociada CSIC, Facultad de Ciencia y Tecnología, Universidad del País Vasco / EHU, P.O. Box 644, Bilbao E-48080, Spain
E-mail: jbermejo@we.lc.ehu.es

A.I. Krivchikov, A.N. Yushchenko, V.G. Manzhelii, and O.A. Korolyuk

B. Verkin Institute for Low Temperature Physics and Engineering of the National Academy of Sciences of Ukraine
47 Lenin Ave., Kharkov 61103, Ukraine
E-mail: krivchikov@ilt.kharkov.ua

M.A. González and M. Jimenez-Ruiz

Institute Laue Langevin, 6 Rue Jules Horowitz, Grenoble F-38042, Cedex 9, France

Received October 20, 2006

The phonon scattering processes in the three solid phases of ethanol are investigated using thermal conductivity, light, and neutron-scattering measurements as well as molecular dynamics simulations on single-crystalline models for two crystalline modifications (fully ordered monoclinic and orientationally disordered bcc phases). The orientationally disordered crystal is found to exhibit a temperature dependence of the thermal conductivity that is remarkably close to that of a structurally disordered solid, especially at low temperatures. This results, together with measurements of Brillouin linewidths as derived from light scattering measurements, emphasize the role of orientational disorder in phonon scattering. The experimental results obtained on polycrystal samples are then discussed with the aid of computer simulations on single-crystalline models of both bcc and monoclinic crystals. Our findings are in good agreement with the wealth of thermodynamic and dynamic data available so far, but at variance with the inferences drawn from inelastic x-ray data on polycrystalline samples, where a common nature for the excitations in all phases is postulated.

PACS: **66.70.+f** Nonelectronic thermal conduction and heat-pulse propagation in solids; thermal waves;
65.60.+a Thermal properties of amorphous solids and glasses: heat capacity, thermal expansion, etc.;
61.43.–j Disordered solids;
63.50.+x Vibrational states in disordered systems;
63.20.Ls Phonon interactions with other quasiparticles.

Keywords: thermal conductivity, phonon, light, neutron, scattering, solid ethanol.

1. Introduction

The present understanding of the mechanisms governing heat transport in disordered media rests upon concepts grounded on heat-pulse experiments showing that acoustic phonons, especially those with transverse polarization are the main heat carriers [1]. The lifetime and, therefore, the mean-free-path of such excitations is known to be severely limited due to the action of several scattering mechanisms which are additional to those involved in the dynamics of the phonon gas, which are well established for fully ordered crystals.

One of the most striking findings revealed from work carried out over the last couple of decades, concerns the *quantitative* similarities exhibited by the thermal conductivity of bulk amorphous materials [2] between, say, 0.1 and 10 K, independent of chemical composition. In fact, from the collected data, which now includes a good num-

ber of disordered crystals and quasicrystals [2,3], it is found that the ratio of the wavelength λ of the acoustic wave to the mean free path *l* of all these solids ranges within 10^{-2}–10^{-3}, which suggests the presence of a «universal» behavior of some sort. On such grounds, it is becoming increasingly clear that the presence of «glassy dynamics» cannot be attributed in full to the absence of static translational long-range order (LRO).

Among the disordered crystals quoted above, some molecular or ionic materials in which the constituent particles have random static orientations while their centers of mass sit at the nodes of a three-dimensional crystalline lattice, are also known to exhibit glass-like excitations. Among those, solid ethyl alcohol is perhaps the most convenient benchmark to carry out a quantitative comparison of the effects brought forward by the complete lack of LRO [4] on the property, most sensitive to the propagation of excitations, i.e., the thermal conductivity. The material, apart from the well known *Pc* monoclinic crystalline (fully ordered, $Z = 2$, FOC) modification, can be prepared in three long-lived (although metastable) phases, viz., an amorphous solid or glass, an orientationally-disordered crystal (ODC) or orientational glass showing static orientational disorder but having translational LRO since the molecules sit at the nodes of a bcc lattice, and a crystal with dynamic orientational disorder (rotator-phase crystal or RPC) which retains LRO as a bcc lattice still exists. Two calorimetric glass transitions take place over about the same range of temperatures close to 97 K and correspond to the canonical glass→supercooled liquid and a rotational freezing transition ODC→RPC [4], which is well understood as a purely dynamic phenomenon (see M. Jimenez-Ruiz *et al.* in Ref. 4).

Here we report on measurements of the thermal conductivity of ethyl alcohol for all the solid phases as well as on measurements of the acoustic phonon lifetimes as determined by means of optical Brillouin scattering. Our aim in pursuing such a route is twofold. First and foremost, as stated in a recent review [2] the measurements provide additional tests on the claims of quantitative «universality» of the heat propagation properties at low and intermediate temperatures in disordered matter brought forward by a class of materials for which no data were available in Ref. 2. On a more fundamental vein, our study also aims at verifing recent claims concerning high-frequency (THz) acoustic excitations sampled in disordered matter by means of inelastic x-ray (IXS) or neutron scattering (INS) [5,6]. More specifically, our results may contribute to clarify whether the spectral feature characteristic of the INS or Raman spectra of most glasses usually referred to as the «Boson peak» can be taken as a signature of the high-frequency limit beyond which acoustic excitations become localized as proposed by some authors [5,6], or contrary to that, phonons may propagate down to microscopic scales without having their lifetimes limited by strong scattering processes, as known to be the case for excitations up to GHz frequencies. In this respect, here we will particularly focus onto some details concerning the nature of the spectral response observed by IXS on polycrystals of the same material [7], for which two rather different interpretations have been proposed [6,7]. To the ends just delineated, we complement the experimental study with calculations of the phonon frequencies and linewidths for both the FOC and ODC carried out by means of molecular dynamics simulations on single-crystalline models of both materials using various intermolecular potentials [8]. In doing so we will follow the evolution of the coherent dynamic structure factor $S(Q,E)$ accross the first Brilloin zone deriving unambiguous estimates for the phonon frequencies and inverse lifetimes, an exercise which cannot be pursued in polycrystalline samples as known since long [9]. Such calculations are complementary to previous harmonic lattice dynamics results on the *Pc* monoclinic phase carried out for a semi-rigid model which incorporates the low-lying molecular modes and has been tested against thermodynamic (i.e. specific heat data up to 30 K) and spectroscopic data such as the frequency distributions as derived from neutron scattering as well as Raman spectral data. For more details in this particular aspect the interested reader is referred to Ref. 10.

2. Experimental and computational details

Thermal conductivity measurements [11] were carried out under equilibrium vapor pressure at 2–159 K by the steady-state potentiometric method using a special setup [12]. The preparation of the glass, disordered crystal, or fully ordered monoclinic phase was carried out using previously described procedures [4].

Brillouin light-scattering measurements were carried out using a multipass tandem Fabry–Perot interferometer from about 5 K up to 160 K in backscattering geometry on both glass/liquid and ODC/RPC phases. Measurements on the monoclinic modification were hampered by the strong speckle patterns arising from the sample.

Neutron inelastic scattering experiments were performed using the MARI spectrometer at ISIS (Rutherford Appleton Laboratory), at an incident energy of 15 meV and a temperature of 10 K on fully deuterated samples. Different sample states were prepared *in situ*, the transformation between them monitored by means of diffraction measurements. Additional measurements on the Boson peak were carried out using the IN14 triple axis spectrometer at the Laue–Langevin Institut.

Molecular dynamics simulations were carried out using a semi-flexible representation of the molecules, their predictive capabilities are described in Ref. 8.

3. Results

A summary of the thermal conductivity measurements of the FOC, ODC and RPC phases is shown in the Fig. 1. A glance to such a figure shows that the thermal conductivity of the FOC phase exhibits a shape much like that of most crystalline solids explored so far. From melting ($T_m = 159$ K) down to around 27 K, the thermal conductivity follows the exponential relation $\kappa(T) \propto \exp(-E/T)$ with $E = (38.3 \pm 0.9)$ K. The maximum is at $T = 12$ K; below 4.5 K it then decreases following the well-established $\kappa(T) \propto T^2$ behavior. Notice the abrupt decrease in thermal conductivity by 42% in a narrow temperature interval.

Both ODC and glass exhibit a temperature dependence of $\kappa(T)$ quite similar to that of most amorphous solids [2]. The thermal conductivity increases with temperature at the maximum rate registered below 4 K. A smeared out «plateau» then follows within 5–10 K, above which $\kappa(T)$ experiences a further increase. Such an increase lasts up to $T = 50$ K, from where $\kappa(T)$ for both samples shows a very weak dependence on temperature up to both glass-transitions close to $T_g \simeq 97$ K. The data for ODC closely follows those of the amorphous solid. The thermal conductivity of ODC exceeds that of the structural glass by about 2% at 2 K, 8% at 3.2 K, 16% at 10 K 12% at 25 K and 85% above 50 K. At temperatures beyond T_g our data shows that $\kappa(T)$ for the supercooled liquid and for RPC are both independent of temperature, its value being close to that of liquid ethanol at the temperature of solidification, $T_m = 159$ K.

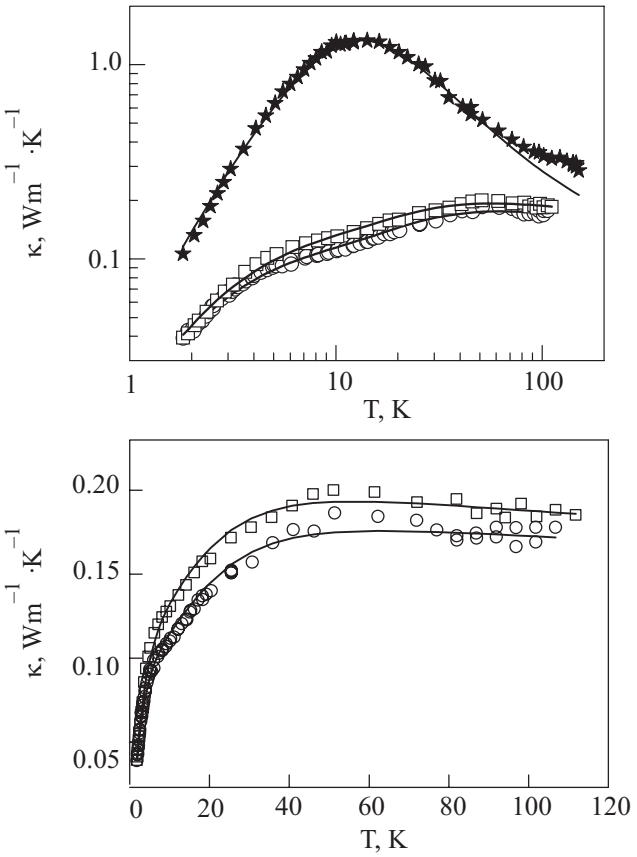

Fig. 1. The upper frame depicts measured thermal conductivities for FOC (stars), ODC (squares), and glass (circles). Solid lines are model fits as described in the text. The lower frame depicts data for glass (circles) and ODC (squares) plotted on a linear scale.

The data has been analyzed on phenomenological grounds by means of the model of soft potentials [11], where phonon scattering is pictured as caused by low-energy excitations such as tunneling states, classical relaxors and soft quasiharmonic vibrations. As the most relevant parameters derived from fitting $\kappa(T)$ to such a model, one gets estimates for the dimensionless tunneling strength C as well as the quantity W which characterizes the crossover from the regime dominated by phonon scattering by low-energy excitations (tunneling states and classical relaxors) to another one dominated by scattering by soft quasiharmonic vibrations. The numerical values are $8.0 \cdot 10^{-4}$, $8.6 \cdot 10^{-4}$ and $4.5 \cdot 10^{-4}$ for C in glass, ODC, and FOC, respectively, and 3.6, 4.0, and 14.0 K for W in the same three phases. In other words, both the tunnel strength and the crossover energy are very close in glass and ODC but differ substantially from that in the fully ordered crystal.

From the strength parameter C we derive the ratio of the acoustic wavelength to its mean-free-path (the relationship given by Pohl *et al.* [2]), a value for the ratio of the wavelength of the acoustic wave to its mean-free-path is derived,

$$\frac{\lambda}{l} = \pi^2 C, \tag{1}$$

and yields figures $\simeq 8 \cdot 10^{-3}$, which is in quantitative agreement with the data reported in Ref. 2 and thus lend further support to the claim of «universality» since it is shown to be apply to this class of materials. Notice that the estimate for the monoclinic crystal is by an order of magnitude larger and thus is well outside the characteristic limits of disordered matter.

A direct experimental way to assess the findings just quoted is provided by measurements of the phonon frequencies and linewidths by Brillouin light-scattering spectroscopy. Notice that for a disordered solid, it is within the limit where the concept of phonon retains its physical meaning, having a well-defined phonon wavevector. This comes as a consequence of the fact that at scales where such experiments are typically performed (that is, for wavevectors about 10^{-3} Å^{-1} and frequencies of a few GHz, comparable to those sampled by thermal conductivity measurements), the solid behaves as an elastic continuum where acoustic excitations exhaust the fre-

quency spectrum. In other words, high-frequency excitations of molecular reorientational origin hardly contribute to spectrum within this range of frequencies and momentum-transfers.

The experimental spectra consist of a single peak attributable to longitudinal phonons, the transverse component being too weak to be observed. The quantities of interest are here the Brillouin peak frequencies ω_B and the peak widths Γ_B. From these quantities we calculate the fractional frequency shift Δ_B and the ratio of Brillouin linewidth to its frequency Q^{-1} as

$$\Delta_B = \frac{\delta\omega_B}{\omega}; \quad Q^{-1} = \frac{\Gamma_B}{\omega_B}. \qquad (2)$$

Here, the fractional frequency shift is calculated with respect to the datum measured for $T = 5$ K and provides a measure of the shift with temperature of the phonon spectrum, that is an estimate of the temperature coefficient of anharmonicity. In turn, Q^{-1} provides an estimate of the phonon damping in terms of a coefficient of internal friction.

Figure 2 displays a comparison of the evolution with temperature of both Δ_B and Q^{-1} for glass and ODC, the temperatures interval covering most of the range of existence of both solids. The temperature dependence Δ_B for both solids is rather weak below 30–40 K, increasing greatly at higher temperatures. In contrast, the internal friction follows nearly the same quasilinear behavior for both solids up to T_g. Both measures of anharmonic interactions are in the two solids remarkably close, which means that the phonon scattering processes operative in both disordered systems are basically the same, in agreement with the thermal conductivity results described above. These results are in agreement with the expectation of a far less anharmonic behavior at low frequencies for FOC. In fact, macroscopic estimates of the γ_{-3} Grüneisen coefficient (see H.E. Fischer *et al.* in Ref. 4) for low frequencies are 2.9, 4.0, and 4.4 for FOC, ODC, and glass, respectively.

To understand the origin of the differences between the two crystals, we carried out a number of molecular dynamics simulations on models of both ODC and FOC single-crystals using the potentials and algorithms already tested against experimental data [8]. The calculated dynamic structure factors along the main (001, 010, and 100) crystal directions and temperatures 5 to 30 K were analyzed in detail. An example of these results is shown in Fig. 3. The lowest temperature (5 K) corresponds to the upper limit of the steep rise of $\kappa(T)$, $T = 30$ K is the limiting temperature where the Debye model is able to account for the measured specific heat [10], or, into other words, where the specific heat can be fully accounted for in terms of acoustic excitations only. Finally, $T = 100$ K comes

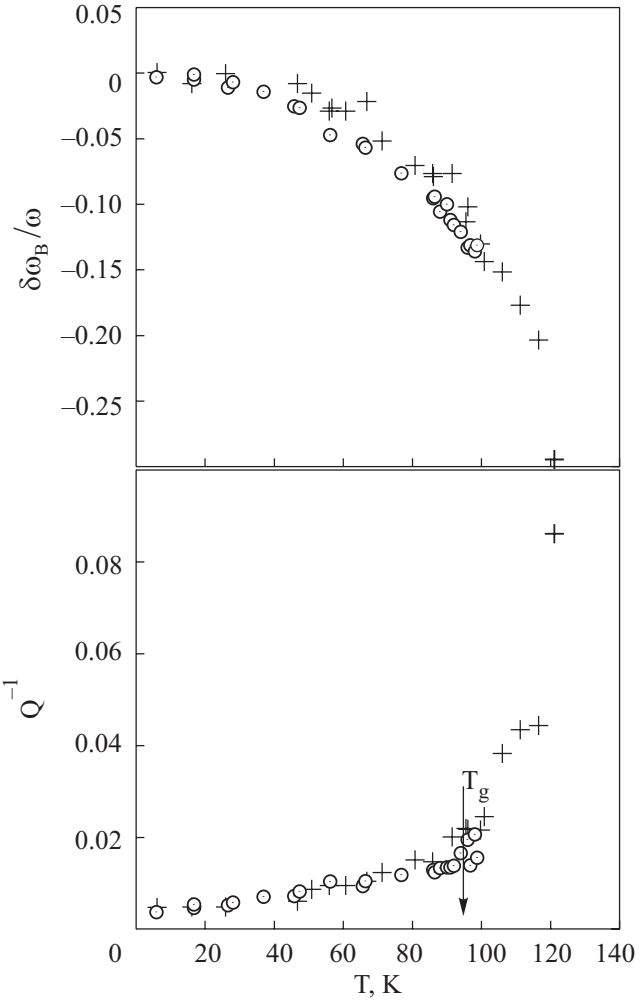

Fig. 2. The measured temperature dependence of the fractional change in sound velocity (the upper frame), and the ratio of linewidth total requency (the lower frame) for ODC/RPC (circles with a dot) and glass/liquid (crosses).

close to the stability limit of ODC and also to the actual temperature where IXS measurements were conducted.

The simulation data for ODC show that for $T > 5$ K only the longitudinal acoustic phonon survives the strong scattering processes due to orientational disorder. The graphs in the upper frame of Fig. 3 for $T = 30$ K depicts the longitudinal branch that corresponds to a hydrodynamic sound velocity of 2639 m·s^{-1}, which produses a well-defined peak within the entire Brillouin zone. The damping of this excitation is subquadratic in wavevector, the linewidth being well approximated by $\Gamma_Q = 9.8\, Q^{3/2}$. A transverse excitation also appears within the first two Brillouin zones. Its linear dispersion corresponds to a propagation velocity of 989 m·s^{-1} while its large damping is follows a stronger than quadratic dependence, $\Gamma_Q = 7.9\, Q^{5/2}$. Increasing the temperature well above the plateau in $\kappa(T)$ has a scaruty effects on the frequency of the longitudinal phonons while its damping increases up to

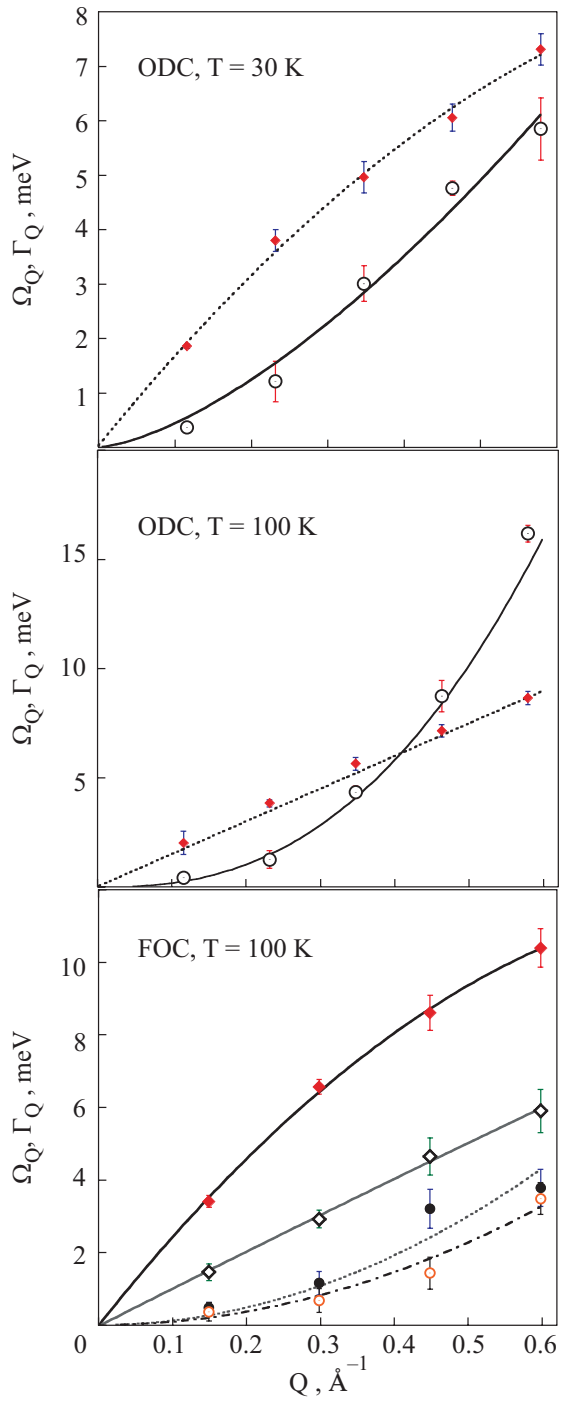

Fig. 3. Calculated phonon frequencies, Ω_Q and phonon linewidths Γ_Q along the (001) direction. The upper frame compares data for the orientationally disordered crystal (ODC) at moderate (30 K) temperature. Filled lozenges and open circles-with-a-dot show dispersion frequencies and damping terms for the longitudinal phonon at 30 K. The lower and middle frames compares data for the FOC and ODC crystals at high temperature (100 K). Longitudinal and transverse phonon frequencies for the FOC are shown by filled and open lozenges, respectively. The corresponding linewidths are depicted by filled and open circles. Lines drawn through the points are approximations given in terms of simple power laws (see text).

$\Gamma_Q = 13.9\, Q^{3/2}$. The absence of a transverse acoustic branch at such temperatures is ascribed to scattering on static orientational disorder since, as shown below, such phonons are observable in the high-temperature crystal where low-energy librations are thermally populated. At a higher temperature, explored experimentally, namely, 0.88 T_g, the longitudinal mode frequencies in ODC are substantially broadened. They, as shown in the lower frame of Fig. 2, correspond to a hydrodynamic value for the sound velocity of 2349 m·s^{-1}, a result in agreement with light-scattering findings [4]. In addition, the phonon remains well defined up to wavevectors corresponding to one half of the Brillouin dimension and the damping coefficient follows the relation $\Gamma_Q = 62.40\, Q^{5/2}$. Data for the monoclinic crystal, also depicted in Fig. 2, reveal a longitudinal branch with a hydrodynamic limiting value of 3917 m·s^{-1} together with a transverse mode propagating with a hydrodynamic velocity of 1574 m·s^{-1}. The damping of both modes is consistently discribed by hydrodynamic Q-dependences with coefficients of 11.98 Å^2·meV and 9.10 Å^2·meV, respectively. Our data conflict with the interpretation of IXS data on polycrystals [7]. The technique, as pointed out recently [6], samples mostly inhomogeneus spectra coming from excitations of non-acoustic nature [10], which pre-empts the interpretation of maxima and linewidths of the spectral bands in terms of physical frequencies and their damping.

4. Discussion and conclusions

As a starting point of the discussion let us consider the signature of static correlations for all phases of ethanol as measured by means of neutron diffraction [4]. Figure 4

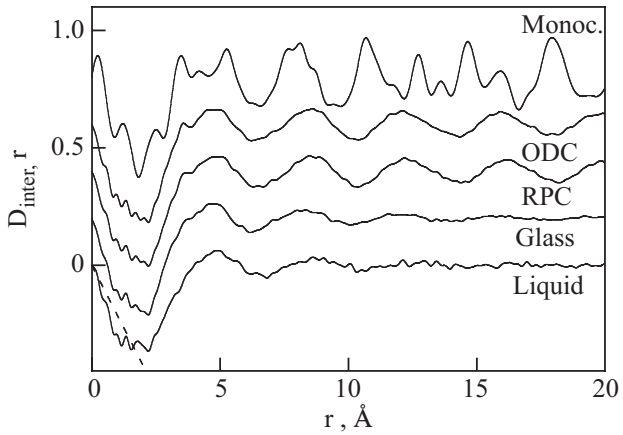

Fig. 4. Experimental intermolecular static correlation functions $D(r) = 4\pi\rho r[g(r) - 1]$ derived from neutron diffraction measurements for all condensed phases after subtraction of the molecular form-factor. Data for the monoclinic crystal and ODC have been measured at 5 K. Data for the liquid were taken at $T = 180$ K and for RPC, at $T = 105$ K. The dotted line is $-4\pi\rho r$, where ρ is the number density. Graphs are displaced 0.2 units upwards to avoid overcrowding.

displays a set of intermolecular static correlation functions corresponding to all phases, including the normal liquid. As expected, the figure shows a close resembance between static correlations in liquid and glass phases as well as that existing between RPC and ODC. It is interesting enough, that the main differences between the functions corresponding to the disordered crystals and those for the liquid/glass states pertain to sustained oscillations with a period $p = 2\pi / Q_p$, where Q_p is the momentum transfer where the main bcc reflection is located. Notice, however, that the relative phases of such oscillations in both fully disordered and bcc samples remain, irrespective of the presence of an underlying lattice.

By contrast, the data pertaining to the fully ordered crystal show a far more complex pattern, which gets out-of-phase with those of the disordered crystals for distances beyond the first coordination sphere, that is, above 6 or 7 Å. Here a molecular orientational ordering is due to strong electrostatic and packing effects, which are not expected to differ much between ODC and FOC. One would then expect that the excitations involving librational molecular motions would bear some resemblance in both crystals.

The lattice dynamics for the monoclinic crystal is well understood for frequencies up to about 25 meV in terms of a semirigid molecular model [10]. The calculated frequency distributions compare favourably below this frequency threshold with those derived from neutron scattering for the fully hydrogenated or deuterated samples [10]. The lattice dynamics model yields a set of 32 dispersion branches. Among these, the acoustic modes are confined below about 8 meV, above which lies a dense mesh of mildly dispersive modes. It was found that purely acoustic modes dominate the frequency distribution below 4.2 meV and the first well-defined peak appearing around 6 meV has already an essentially optical character. The latter becomes predominant above 9 meV. In turn, rotational and librational motions in the bcc crystal have been considered in detail (see Criado *et al.* in Ref. 4) and found to correspond to reorientations amongst 24 different basic orientations set by the crystal site and molecular point symmetries. The frequency distribution of such motions covers a wide range extending up to about 20 meV. Furthermore, as shown by H.E. Fischer *et al.* [4], the frequency spectra for both glass and ODC are remarkably close and show below 5 meV the characteristic excess modes of glassy matter. By comparison, the first van Hove singularity that corresponds to zone boundary transverse acoustic phonons is still seen at 80 K. Subsequent analysis of the spectral distributions for glass, ODC, and FOC in terms of frequency moments $< \omega^n >$ has shown how the lower order moments (up to $n = -1$), related to low frequencies and are thus pertinent for glass

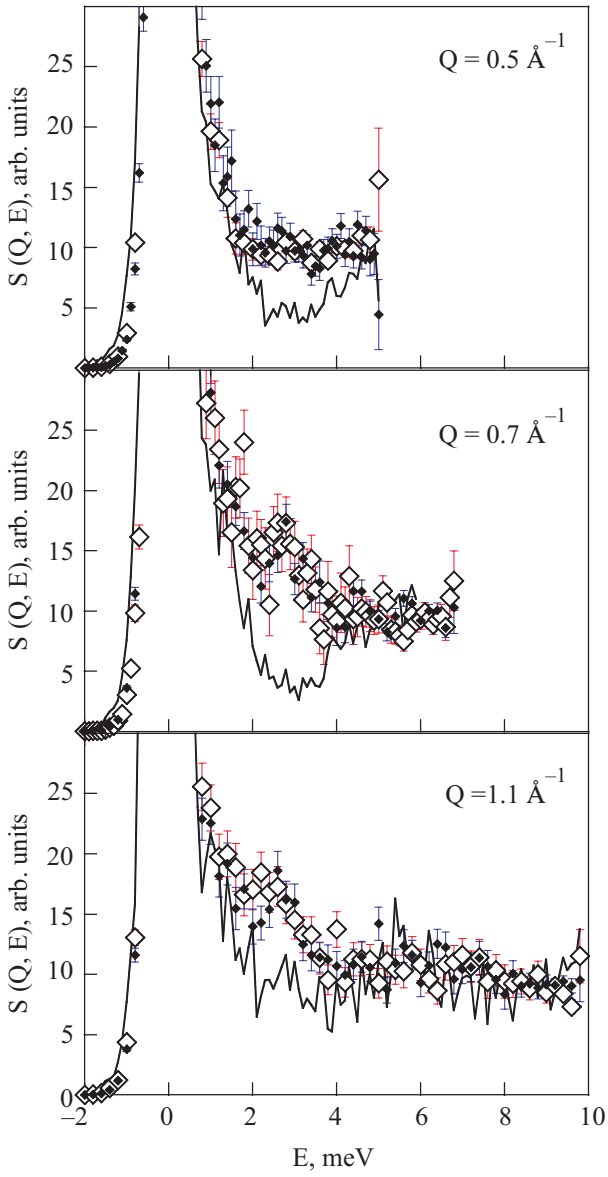

Fig. 5. Inelastic neutron scattering spectrum for fully deuterated glassy (filled symbols) ODC (open symbols) and FOC (solid line) ethanol measured at $T = 10$ K.

physics, for both glassy phases differ from that for the FOC, while the higher order moments which come from higher frequencies, become increasingly close for all the three phases. These facts help understand the close similitude of the results for glass, ODC, and FOC reported in Ref. 7. This similarity is a consequence of the closely related spectra of molecular orientational modes in all the three phases, which dominate the frequency range explored by the IXS technique. However, the spectra for the glassy phases become strinkingly different from that of FOC within the frequency range dominated by the acoustic modes as Fig. 5 exemplifies. In other words and to put things explicitly, the results in Ref. 7 are to be taken as descriptive at best since the analysis, in which all IXS inten-

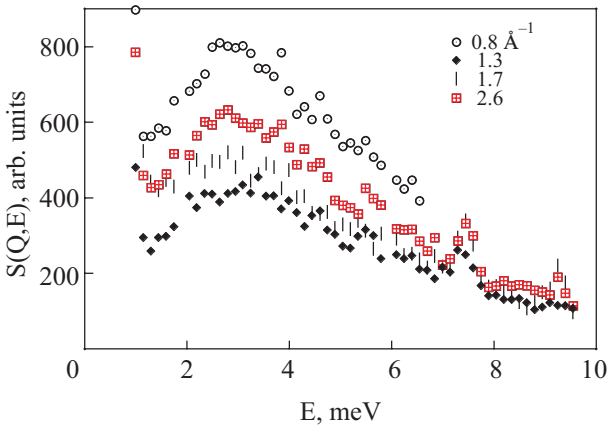

Fig. 6. Inelastic neutron scattering spectrum for ODC ethanol measured at $T = 10$ K and several momentum transfers as well as frequency, covering the Boson peak. The peak at about 7.4 meV is spurious.

sities below 22 meV are described in terms of a single physical frequency, is not meaningful.

Our final remark concerns the current debate on phonon localization due to disorder [5]. What we discuss is: can the propagation of acoustic excitations in glassy matter take place beyond a spectral feature located at low frequencies known as the Boson peak. Its origin still is unclear, but is known to be related to the hump that appears in the specific heat if plotted as C_p / T^3. Studies on vitreous silica [6] seem to indicate the existence of a crossover region well inside the first pseudo-Brillouin zone, that is, for $Q < Q_p / 2$ where the excitation linewidths compare with their characteristic frequency and thus cease to propagate. Such a crossover frequency (or wavevector), which is usually referred to as the Ioffe–Regel limit, was identified in some studies as that corresponding to the Boson peak. For the materials under discussion here we show in Fig. 6 the shape of the low-frequency spectra for several momentum transfers values. Such a feature appears as a well-defined peak centered at about 3 meV, showing no clear Q-dependence of its frequency or width. Its thermodynamic correlative is the hump at $T = 7$ K in the specific heat [10].

Now we address the same issue as above by comparing simulation data depicted in Fig. 3 with the spectra, showing the Boson peak, in Fig. 6. Because simulations dealt with a single crystal, the frequencies and linewidths of acoustic phonons cane tracked down up to the Brillouin zone boundary. Data for ODC at the lowest temperature (5 K) shows no indication of a crossover in the Ioffe–Reggel sense and, therefore, one would expect that longitudinal acoustic phonons propagate within the Brillouin zone. By contrast, data for $T = 100$ K do show a crossover in ODC at about 0.4 Å^{-1}. The inference such a comparison allows us to make tells that thermal disorder seems to be more fundamental issue concerning the localization of acoustic waves than its static counterpart. The result that went unnoticed in the current debate is however well known concerning the damping of acoustic phonons in cubic crystals [13], where it is known that the phonon relaxation rate depends on the fifth power of the temperature.

In summary, the concurrent use of thermal conductivity measurements, light scattering experiments, and molecular dynamics simulations on single crystalline models of ODC and FOC solids has enabled us to establish the prominent role or molecular orientational disorder as the main source of acoustic phonon scattering in disordered matter. As an additional result, our study points towards the important role of thermal effects in the attenuation of acoustic phonons.

The authors are indebted to the Fundamental Research Foundation of Ukraine (Project F-16/1-2006) for a partial support of this study.

The study was partially supported with a Grant of President of Ukraine for young scientists engaged in scientific research (GP/F13/0037).

1. P.D. Wu, J.R. Olson, and R.O. Pohl, *J. Low Temp. Phys.* **113**, 123 (1998).
2. R.O. Pohl, X. Liu, and E. Thompson, *Rev. Mod. Phys.* **74**, 991 (2002).
3. M. Kobas, T. Weber, and W. Steurer, *Phys. Rev.* **B71**, 224206 (2005).
4. M.A. Ramos, S. Vieira, F.J. Bermejo, J. Dawidowski, H.E. Fischer, H. Schober, M.A. Gonzalez, C.K. Loong, and D.L. Price, *Phys. Rev. Lett.* **78**, 82 (1997); A. Criado, M. Jimenez-Ruiz, C. Cabrillo, F.J. Bermejo, M. Grimsditch, H.E. Fischer, S.M. Bennington, and R.S. Eccleston, *Phys. Rev.* **B61**, 8778 (2000); M. Jimenez-Ruiz, A. Criado, F.J. Bermejo, G.J. Cuello, F.R. Trouw, R. Fernandez-Perea, H. Lowen, C. Cabrillo, and H.E. Fischer, *Phys. Rev. Lett*. **83**, 2757 (1999); C. Cabrillo, F.J. Bermejo, M. Jimenez-Ruiz, M.T. Fernandez-Diaz, M.A. Gonzalez, and D. Martin Marero, *Phys. Rev.* **B64**, 064206 (2001); H.E. Fischer, F.J. Bermejo, G.J. Cuello, M.T. Fernandez-Diaz, J. Dawidowski, M.A. Gonzalez, H. Schober, and M. Jimenez-Ruiz, *Phys. Rev. Lett*. **82**, 1193 (1999); M.A. Miller, M. Jimenez-Ruiz, F.J. Bermejo, and N.O. Birge, *Phys. Rev.* **B57**, R13977 (1998).
5. B. Rufflé, M. Foret, E. Courtens, R. Vacher, and G. Monaco, *Phys. Rev. Lett.* **90**, 095502 (2003); O. Pilla, A. Cunsolo, A. Fontana, C. Masciovecchio, G. Monaco, M. Montagna, G. Ruocco, T. Scopigno, and F. Sette, *Phys. Rev. Lett.* **85**, 2136 (2000); F.J. Bermejo, G.J. Cuello, E. Courtens, R. Vacher, and M.A. Ramos, *Phys. Rev. Lett.* **81**, 3801 (1998).
6. B. Rufflé, G. Guimbretiere, E. Courtens, R. Vacher, and G. Monaco, *Phys. Rev. Lett.* **96**, 045502 (2006).
7. A. Matic, C. Masciovecchio, D. Engberg, G. Monaco, L. Borjesson, S.C. Santucci, and R. Verbeni, *Phys. Rev. Lett.* **93**, 145502 (2004).

8. M.A. González, E. Enciso, F.J. Bermejo, and M. Bée, *Phys. Rev.* **B61**, 6654 (2000); M.A. González, E. Enciso, F.J. Bermejo, M. Jimenez-Ruiz, and M. Bée, *Phys. Rev.* **E61**, 3884 (2000).
9. F.W. de Wette and A. Rahman, *Phys. Rev.* **176**, 784 (1968).
10. C. Talón, A. Ramos, S. Vieira, G.J. Cuello, F.J. Bermejo, A. Criado, M.L. Senent, S.M. Bennington, H.E. Fischer, and H. Schober, *Phys. Rev.* **B58**, 745 (1998).
11. A. Krivchikov, A.N. Yushchenko, V.G. Manzhelii, O.A. Korolyuk, F.J. Bermejo, R. Fernández-Perea, C. Cabrillo, and M.A. González, *Phys. Rev.* **B74**, 060201(R) (2006).
12. A.I. Krivchikov, B.Ya. Gorodilov, O.A. Korolyuk, V.G. Manzhelii, H. Conrad, and W. Press, *J. Low Temp. Phys*. **139**, 693 (2005); A.I. Krivchikov, V.G. Manzhelii, O.A. Korolyuk, B.Ya. Gorodilov, and O.O. Romantsova, *Phys. Chem.Chem. Phys*. **7**, 728 (2005).
13. I.G. Kuleev and I.I. Kuleev, *Fiz. Tverd. Tela* **47**, 312 (2005).